

**Unraveling the nanomechanical properties of surface-grafted conjugated polymer brushes
with ladder-like architecture**

Monika Słowikowska^a, Karol Wolski^{a*}, Artur J. Wójcik^a, Daniel Wesner^b, Holger Schönherr^b,

Szczepan Zapotoczny^{a*}

^a *Faculty of Chemistry, Jagiellonian University, Gronostajowa 2, 30-387 Krakow, Poland*

^b *Physical Chemistry I & Research Center of Micro and Nanochemistry and Engineering (Cμ),
Department of Chemistry and Biology, School of Science and Technology, University of
Siegen, Adolf-Reichwein-Str. 2, 57076 Siegen, Germany*

** Corresponding authors*

Supplementary Information

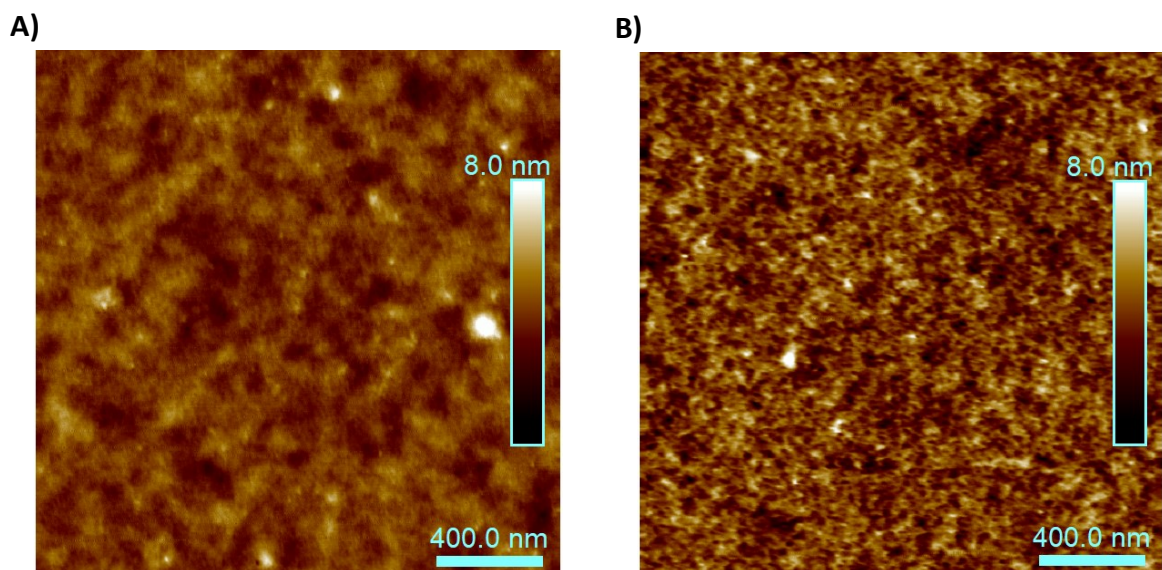


Figure S1. AFM topography images of: A) PTPM_depr_30_SiO₂ and B) PTPM_con_30_SiO₂.

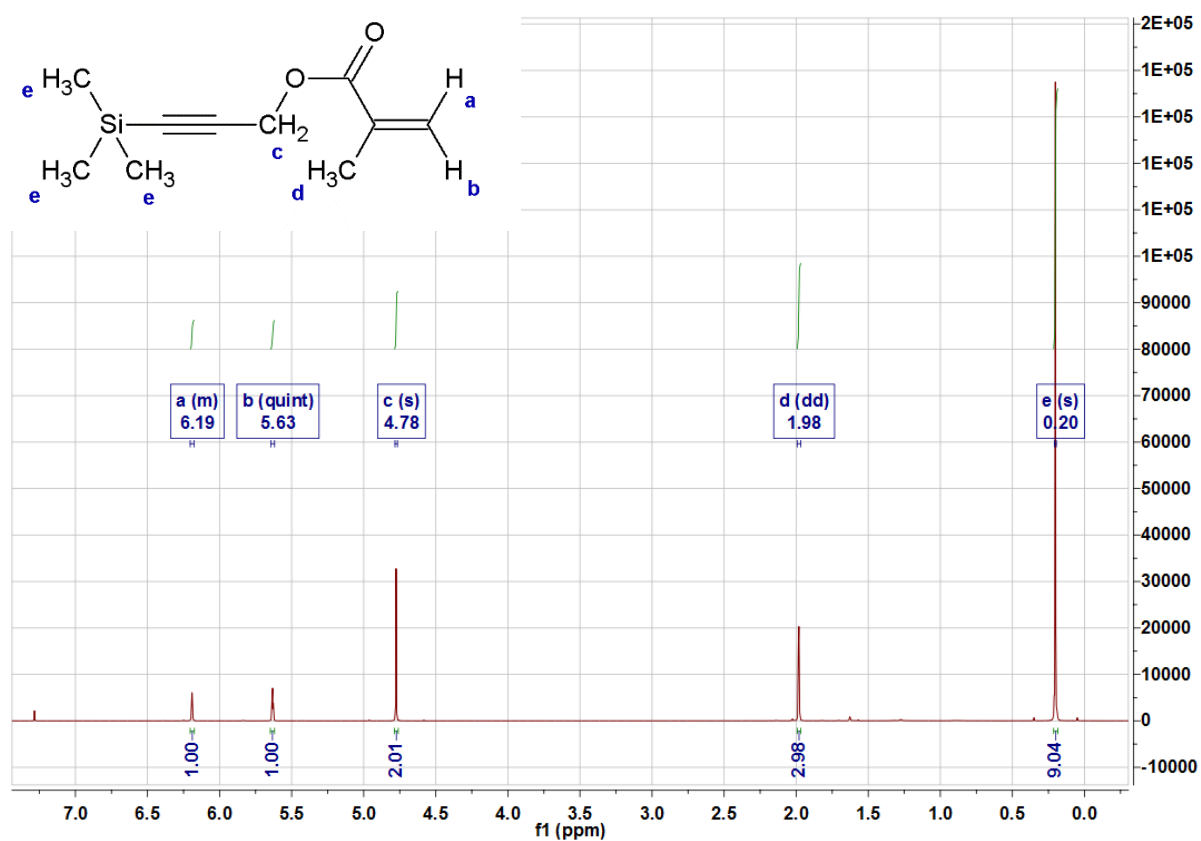


Figure S2. ¹H NMR spectrum of TPM monomer.

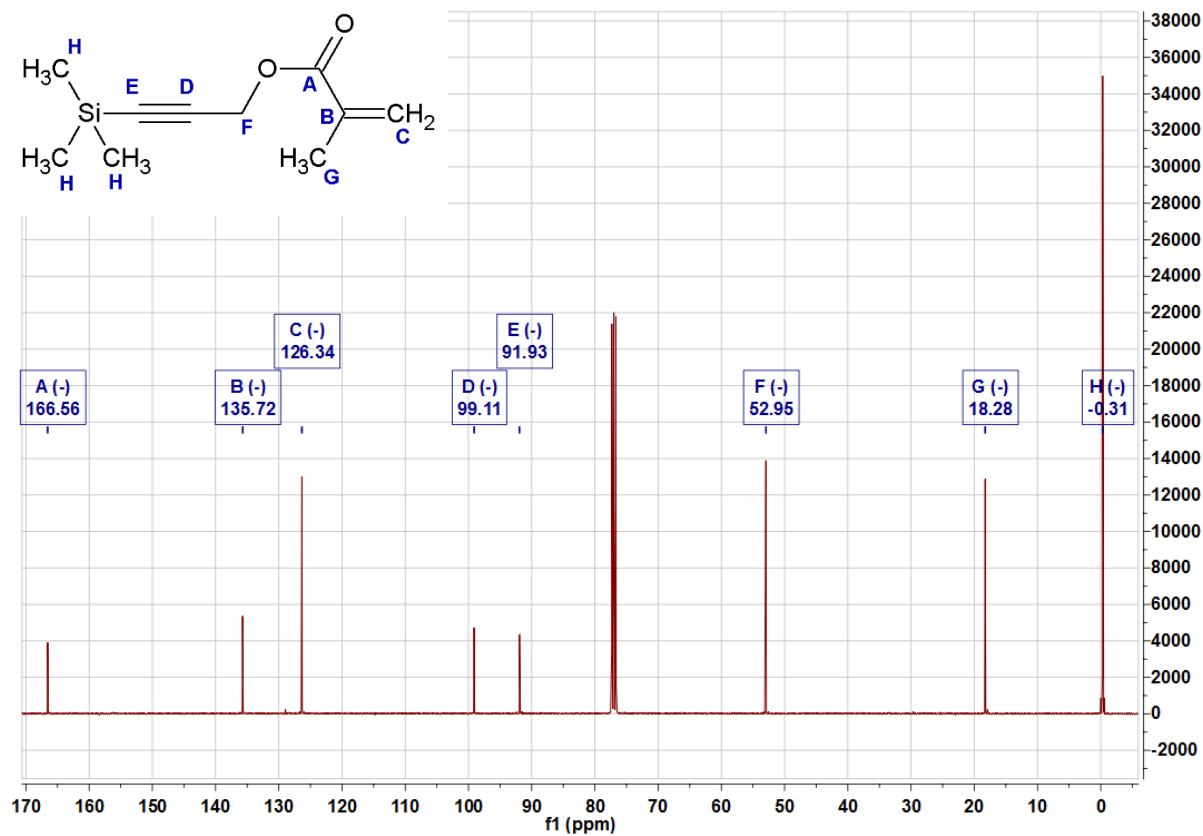


Figure S3. ¹³C NMR spectrum of TPM monomer

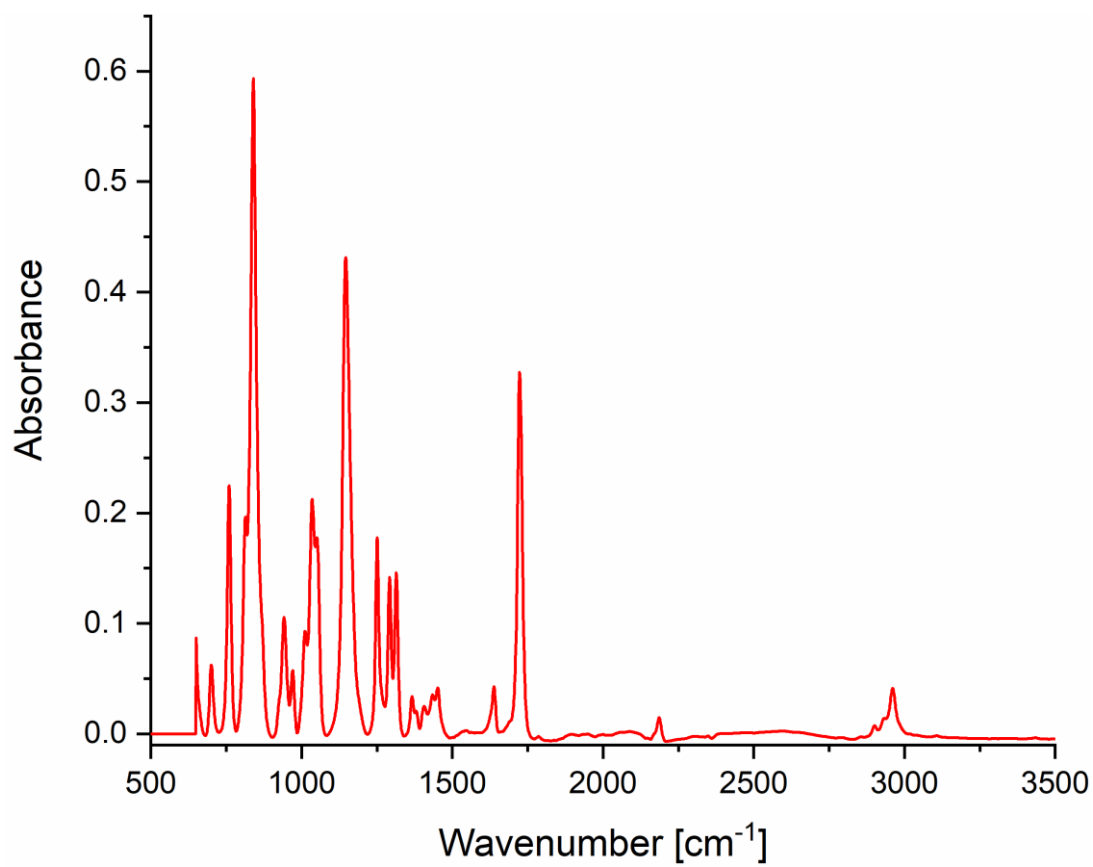


Figure S4. FTIR spectrum of TPM monomer.

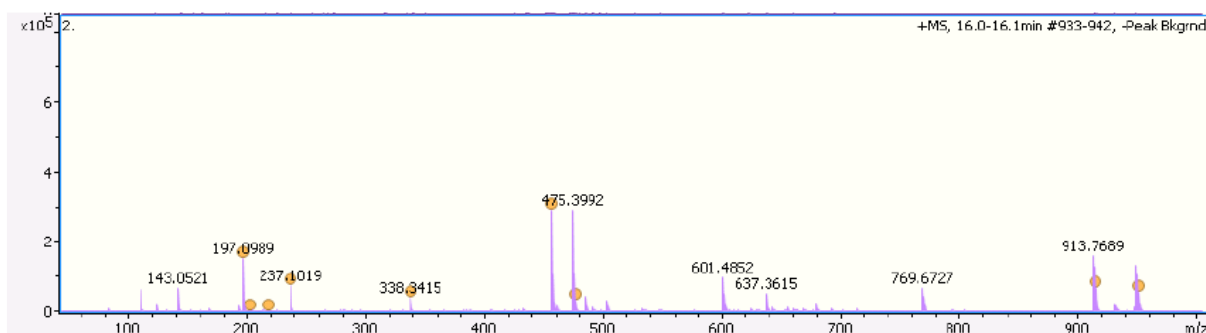


Figure S5. LCMS spectrum of TPM monomer.

FT-IR characterization of PTPM brushes

FT-IR spectrum captured after SI-PIMP (Fig. S6) show the bands characteristic for: CH₂ and CH₃ (C-H stretching vibrations, 2962 cm⁻¹ and 2901 cm⁻¹), protected acetylene group (C≡C stretching vibration, 2187 cm⁻¹), carbonyl group (C=O stretching, 1742 cm⁻¹) and polymer main chain (CH₃, CH₂ deformative and C-C stretching in the region of 1486-1250 cm⁻¹). The FT-IR spectrum after the deprotection step (fig. S6) revealed the appearance of a new characteristic band at 3296 cm⁻¹ (C-H stretching vibrations in C≡C-H) and shifting of the band previously observed at 2187 cm⁻¹ to 2130 cm⁻¹ (C≡C stretching in C≡C-H). The formation of conjugated polyacetylene chains after ST-SIP was supported by greatly decreased intensity of the bands at 3296 cm⁻¹ and 2130 cm⁻¹ and the appearance of a weak broad band above 3000 cm⁻¹ (C=C-H stretching, see Fig. S6).

Surface selection rule in grazing-angle FT-IR in combination with p polarized light shows modes/vibrations with dipole moment orientated along the surface normal direction with enhanced intensity. Interestingly, the intensity of the band at 1150 cm⁻¹ is drastically changing with respect to the intensity of carbonyl band (1740 cm⁻¹) after subsequent modifications (see figure S6). The mentioned band is assigned to the C-O-C stretching vibrations in the ester

group that is a part of the “rung of the ladder”. Thus, the more intense is this band the more perpendicular orientation of the side group is observed. A moderate intensity of the band was observed for the thickest parent brushes, due to stretched conformation of crowded macromolecules related to the presence of bulky trimethylsilyl groups that enforce a parallel orientation of C-O-C groups with respect to the surface (see Fig. S6). After deprotection and hence the removal of 40% of polymer mass, the intensity of the band at 1150 cm^{-1} is greatly enhanced. More free space to be occupied by the side groups is formed allowing more packed, collapsed conformation of the chains with more random orientation of the pendant groups. It is also reflected in quite large intensity of the band at 3300 cm^{-1} (C-H stretching vibrations in the deprotected acetylene group). After self-templating polymerization the intensity of the band at 1150 cm^{-1} is greatly reduced confirming parallel orientation of C-O-C – rung of the ladder. Furthermore, even the carbonyl group may be enforced to adopt a more parallel orientation, due to the crowding of “rungs of the ladder”, as the intensity of the band at 1740 cm^{-1} in the spectrum of ladder-like brushes decreased to 70-75% with respect to the spectra of deprotected and parent PTPM brushes. Such a parallel orientation of side groups is not expected in randomly cross-linked brushes. It is important to underline that dissociation of the ester band could be excluded, as enhanced intensity was observed for the bands assigned to C-H stretching vibrations (2951 cm^{-1}), due to the signal-enhancing orientation of the CH_2 groups that link to acetylene chains ($\text{O-CH}_2\text{-(C=C)}_n$). The presence of ester groups in ladder-like brushes was also confirmed by XPS spectroscopy (Fig. S15)

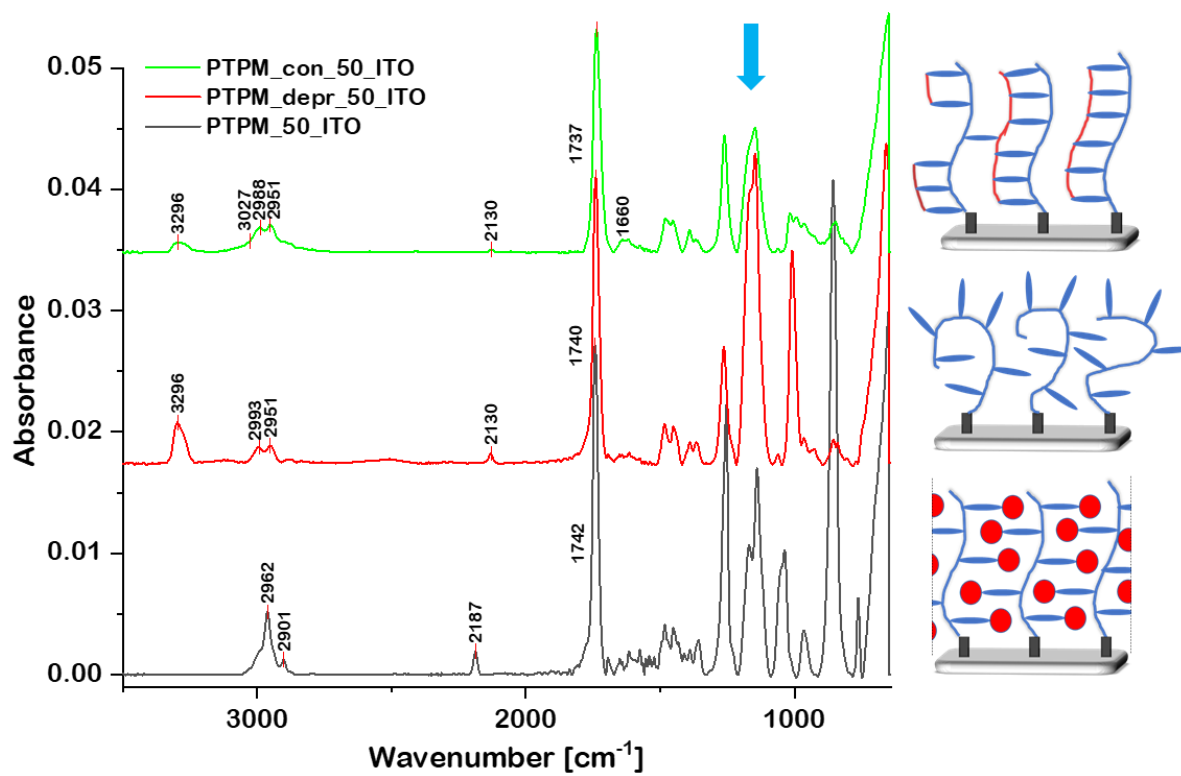


Figure S6. Grazing incidence FT-IR spectra of PTPM_50_ITO after SI-PIMP, deprotection of acetylene groups and self-templating polymerization.

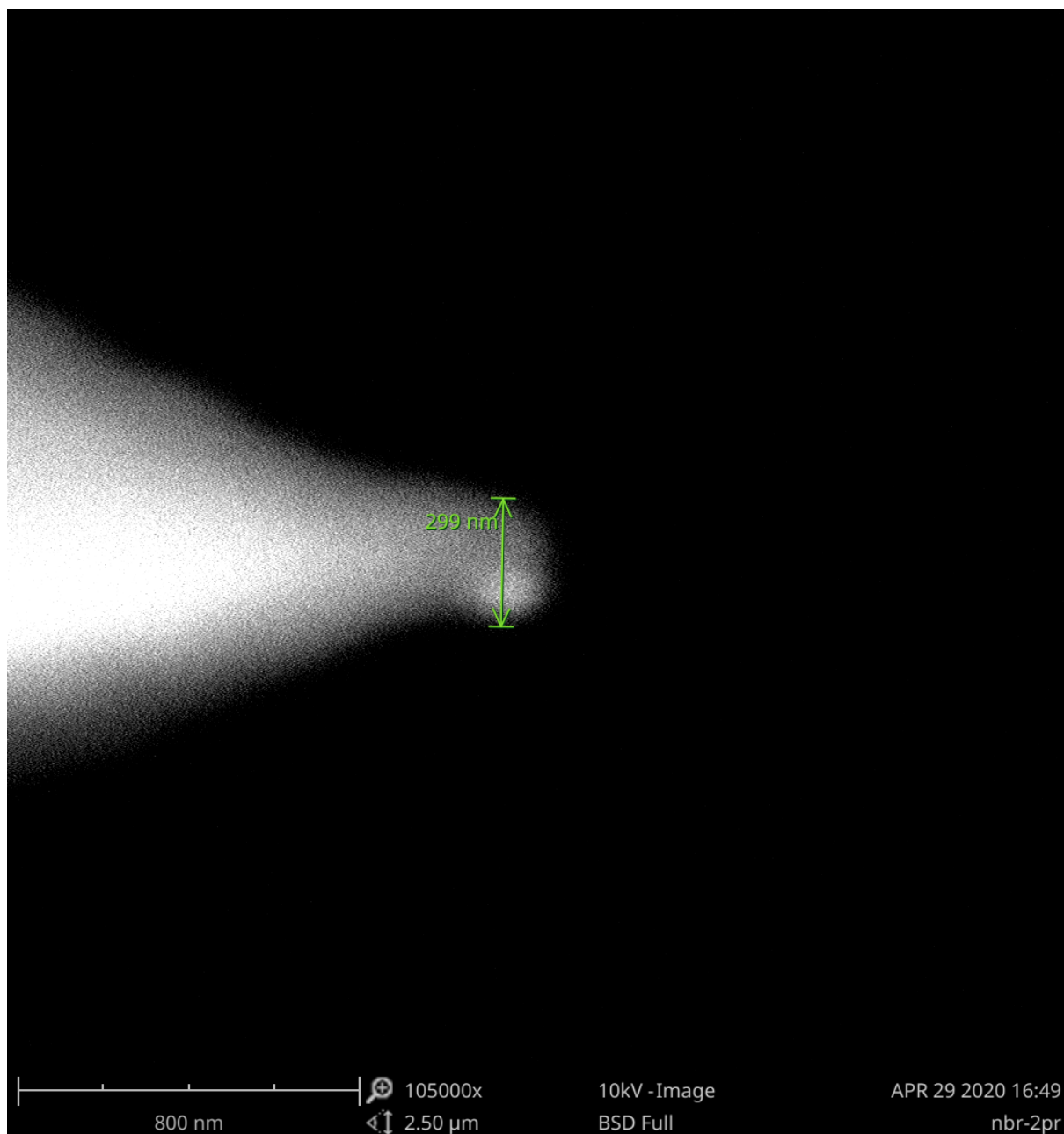


Figure S7. SEM image of DDESP probe used for nanoindentation of PTPM brushes in air.

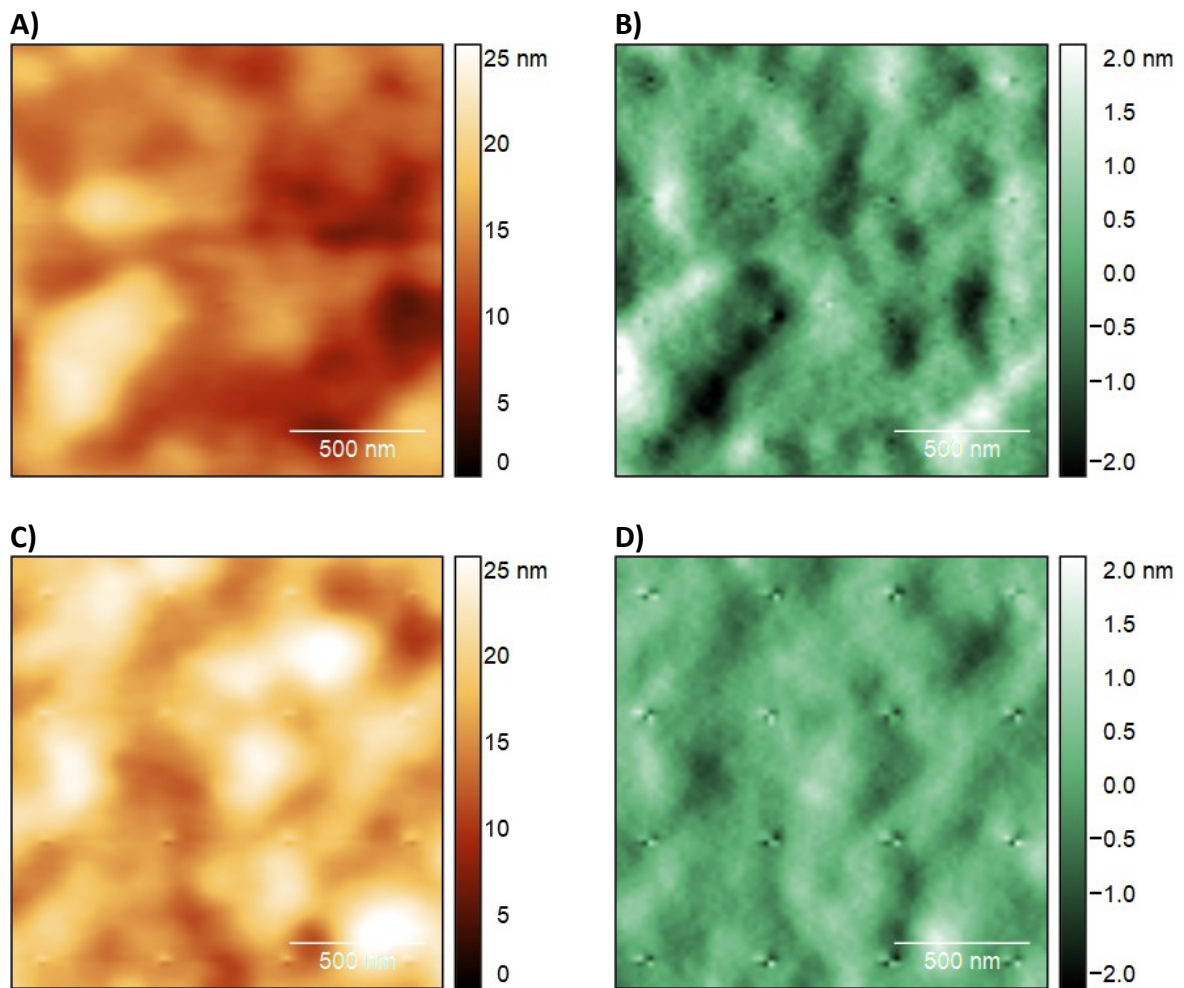


Figure S8. A), C) AFM height and B), D) amplitude images of PTPM_60_ITO after indentation with a sharp tip in air at low (150 nN , A and B) and high loads (700 nN, C and D).

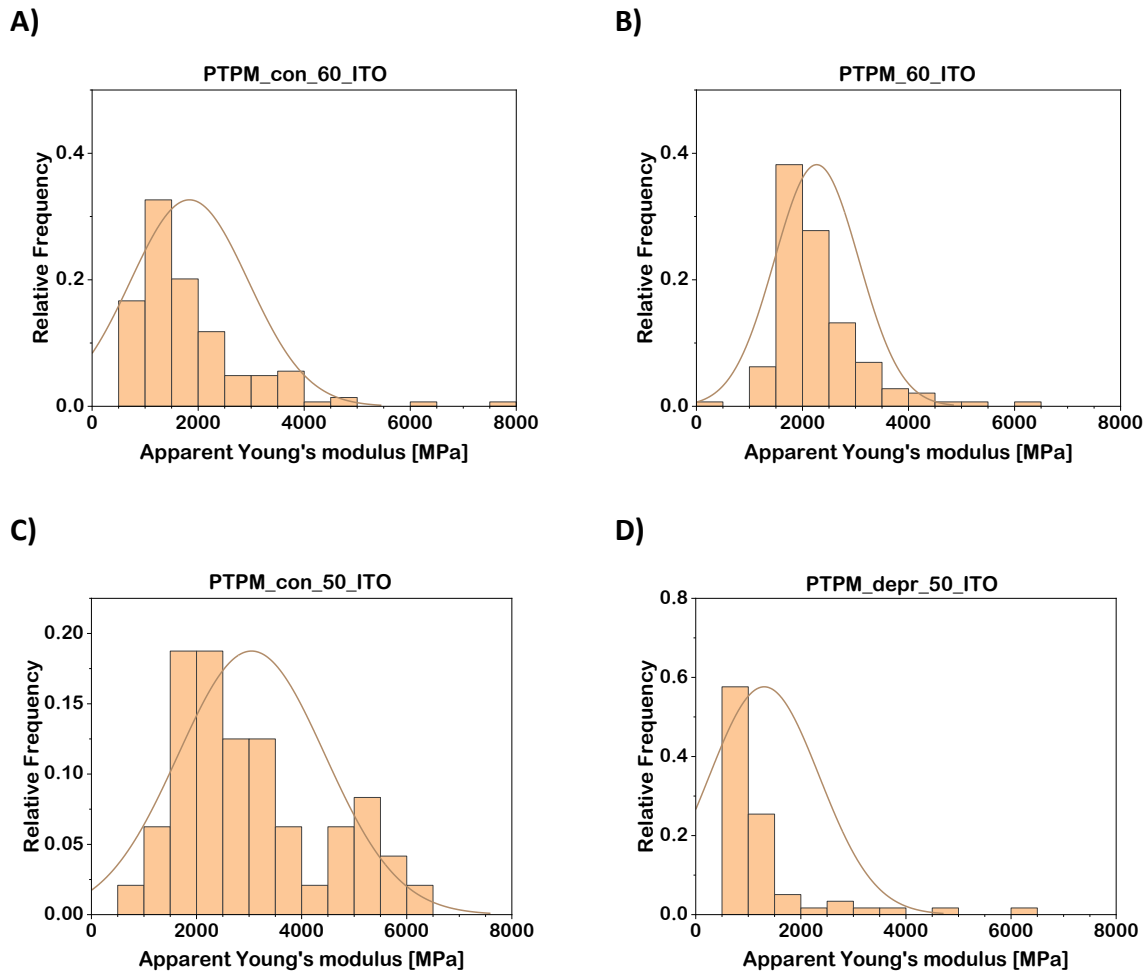


Figure S9. Histograms of distribution of apparent Young's modulus for A) PTPM_con_60_ITO, B) PTPM_60_ITO, C) PTPM_con_50_ITO and D) PTPM_depr_50_ITO. Results were obtained with sharp (A and B, tip radius 7 nm) and dull probe (C and D, tip radius 150 nm).

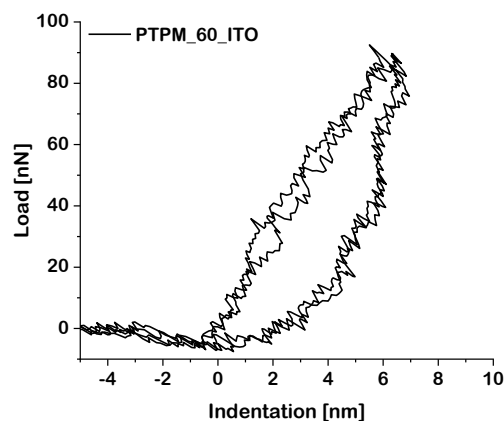


Figure S10. Indentations curves of PTPM_60_ITO measured in air using sharp probes (tip radius 7 nm).

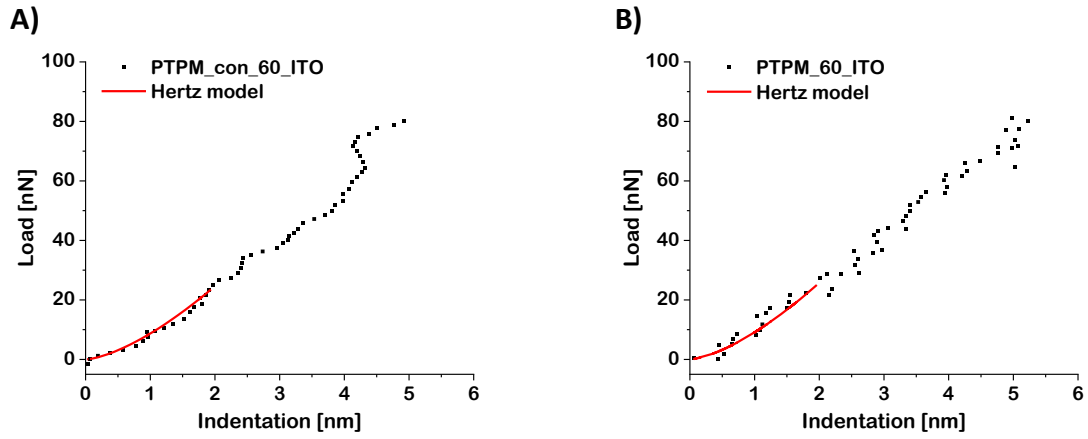


Figure S11. Exemplary approach curves of A) PTPM_con_60_ITO and B) PTPM_60_ITO with fitted Hertz model (measurements performed using sharp probe, tip radius 7 nm).

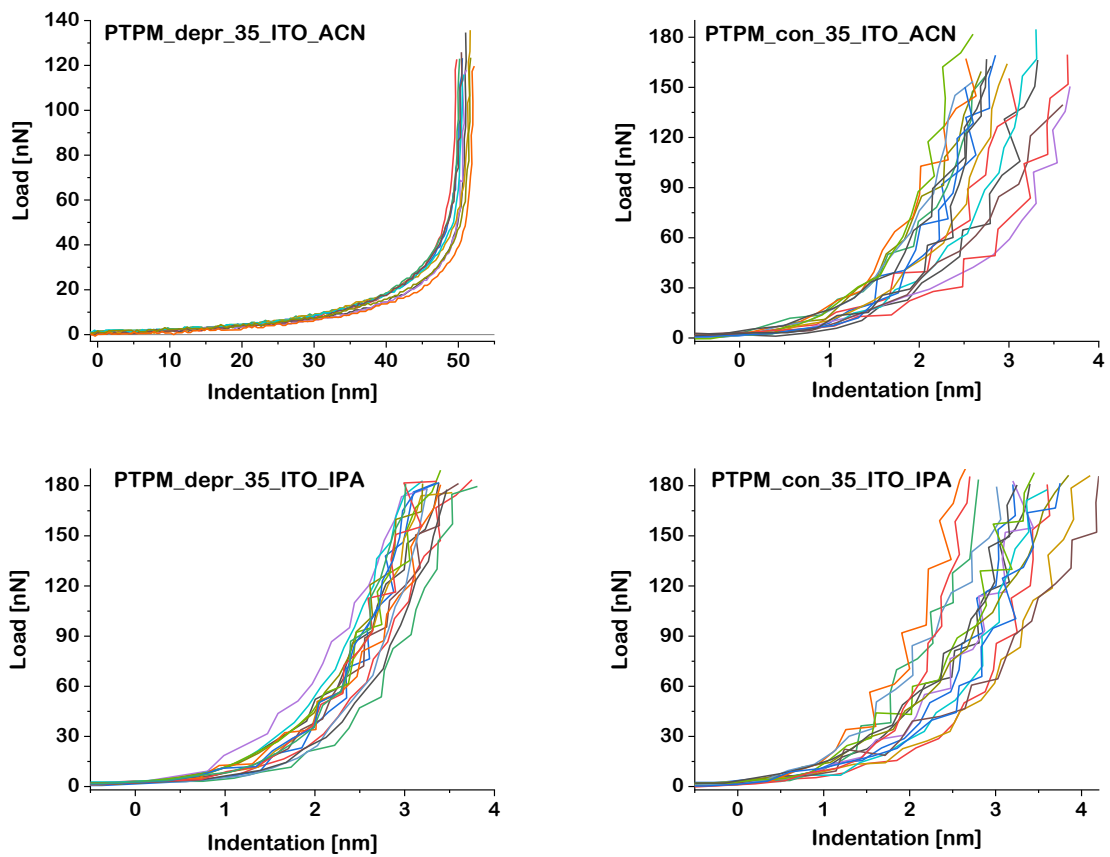


Figure S12. Individual load curves of PTPM_depr_35_ITO and PTPM_con_35_ITO captured in IPA and ACN.

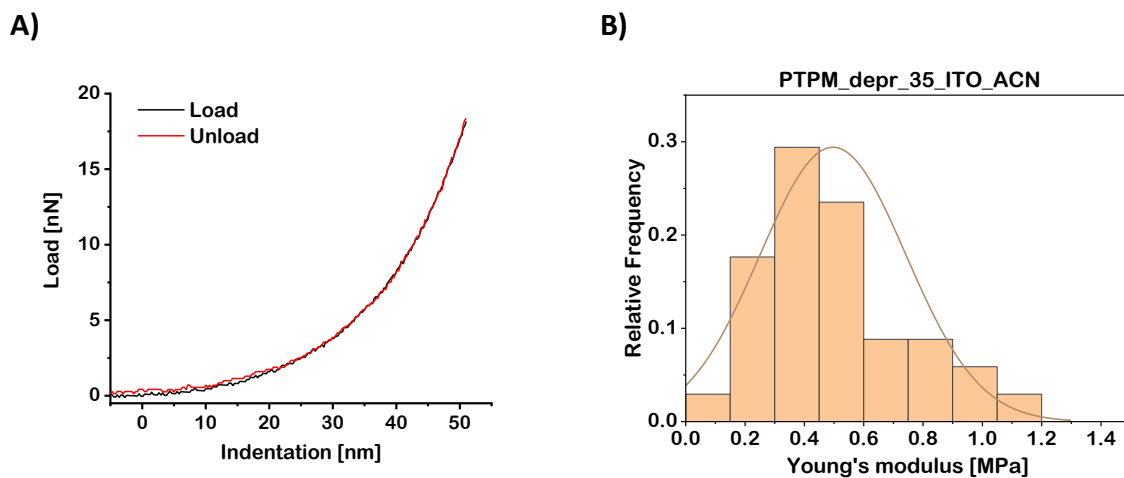


Figure S13. A) Indentation load and unload curves of PTPM_depr_35_ITO in acetonitrile and B) histogram of calculated Young's modulus. Results for soft cantilever equipped with a probe with tip radius of 300 nm.

Table S1. Results of Young's modulus calculations assuming different values of Poisson's ratio.

Sample	Conditions	Young's modulus,	Young's modulus
		[GPa] $\nu=0.5$	[GPa] $\nu=0.33$
PTPM_60_ITO	air	1.9 ± 0.7	2.2 ± 0.8
PTPM_con_60_ITO	air	1.5 ± 0.9	1.8 ± 1.1
PTPM_depr_35_ITO	IPA	1.4 ± 0.3	1.7 ± 0.4
	ACN	$1.5 \times 10^{-3} \pm 5 \times 10^{-4}$ $5 \times 10^{-4} \pm 2 \times 10^{-4*}$	$1.8 \times 10^{-3} \pm 6 \times 10^{-4}$ $6 \times 10^{-4} \pm 2 \times 10^{-4*}$
PTPM_con_35_ITO	IPA	1.2 ± 0.5	1.4 ± 0.6
	ACN	1.4 ± 0.5	1.7 ± 0.6

* Measurements were performed using a softer cantilever (calibrated spring constant equal to 4.4 N/m) and a tip with a radius of 300 ± 10 nm.

Table S2. Calculated values of apparent Young's modulus for different force thresholds.

Sample	Force threshold [nN]	Apparent Young's modulus, [GPa]
PTPM_60_ITO	18	2.2 ± 0.8
	30	2.2 ± 0.5
	70	1.7 ± 0.3
PTPM_con_60_ITO	18	1.8 ± 1.1
	30	1.7 ± 0.7
	70	1.5 ± 0.5

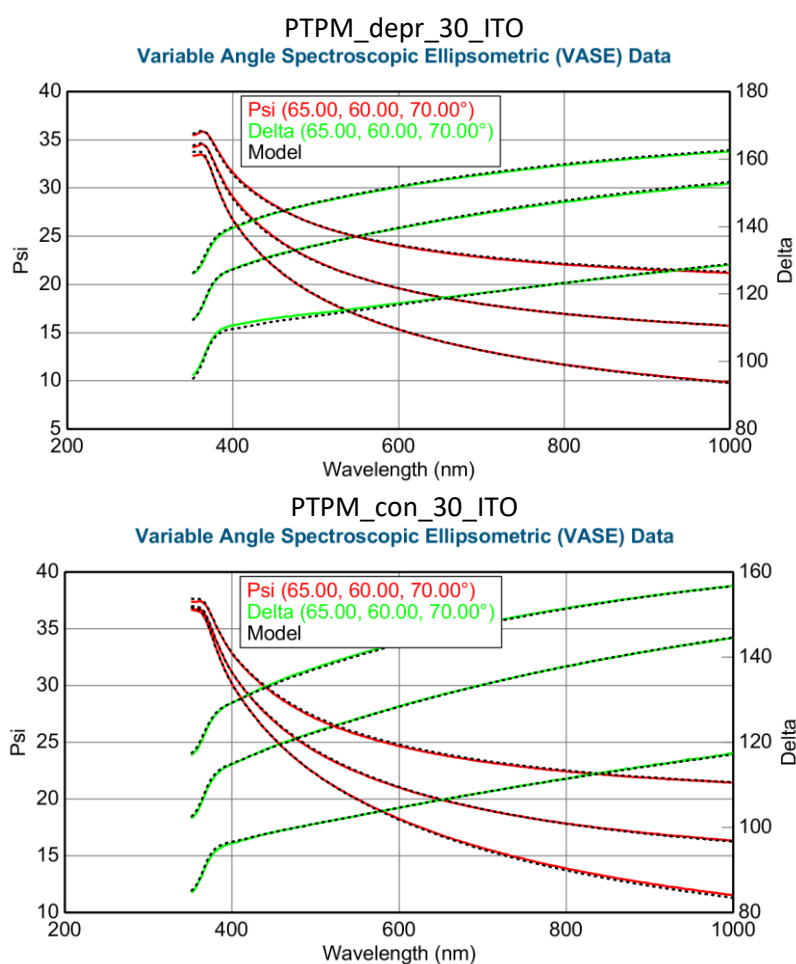


Figure S14. Exemplary ellipsometric data captured for PTPM_depr_30_ITO and PTPM_con_30_ITO.

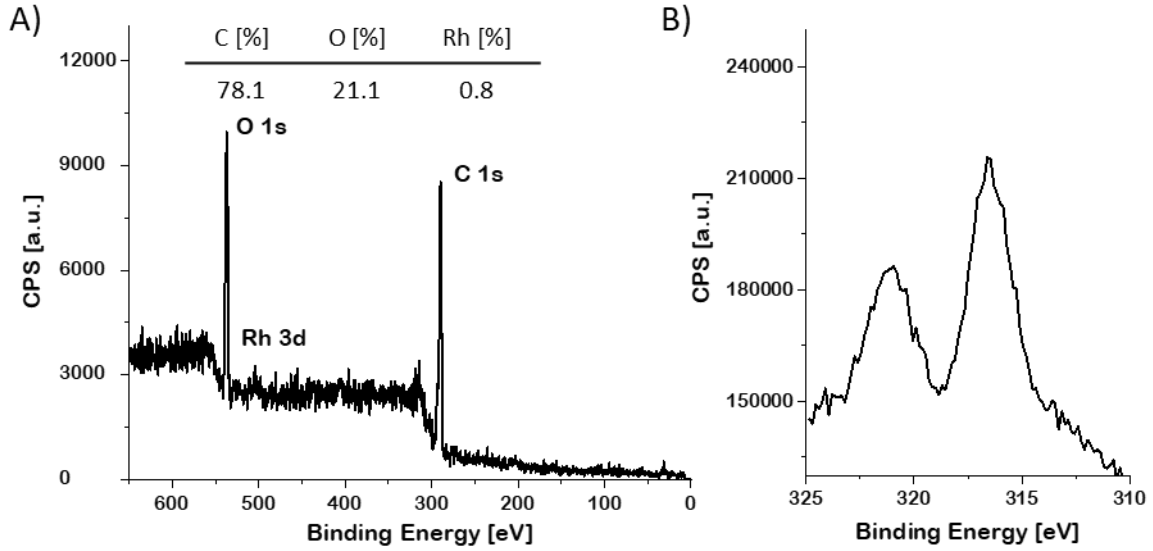


Figure S15. A) XPS survey spectra of PTPM_con_30_ITO. B) Detailed XPS element scan of Rh 3d.

Estimation of grafting density

In order to estimate the grafting density of the PTPM brushes, we have used the methodology described by Benetti et al.¹ that is based on the assumption that the contour length L of surface grafted polymers is comparable to the brush thickness in good solvent h_{wet} . Assuming that methacrylic monomer length equals $l = 0.26 \text{ nm}^2$ one may calculate the molar mass of surface-grafted polymer chains according to Equation 1.

$$M_n = \frac{h_{wet} \cdot M}{l} \quad [1]$$

where M denotes the molar mass of the monomeric unit.

For PTPM_depr_30_SiO₂ the wet brush thickness was found to be 48 nm, while $M = 124 \text{ g/mol}$.

Thus, one may calculate that $M_n = 23800 \text{ g/mol}$, hence the grafting density Σ can be calculated using Equation 2.

$$\Sigma = \frac{h_{dry} * d * N_A}{M_n} \quad [2]$$

where $h_{dry} = 18$ nm is the dry brush thickness, $d = 1.08 \cdot 10^{-21}$ g/nm³ the assumed polymer density,³ and N_A is Avogadro's number.

Assuming that deprotected PTPM has similar polymer density to poly(propyl methacrylate) PPMA,³ which possesses a propyl group instead of propyne (like in PTPM) attached to the methacryloyl group, a value of Σ for PTPM_depr_30_SiO₂ of 0.49 macromolecules/nm² is obtained. Since the grafting density should not vary with chemical modification of the side groups in self-templating polymerization, one may expect a very similar value for PTPM_con_30_SiO₂ as well.

References

-
- ¹ E. M. Benetti, S. Zapotoczny and G. J. Vancso, *Adv. Mater.*, 2007, **19**, 268–271.
 - ² J. Guo, P. André, M. Adam, S. Panyukov, M. Rubinstein and J. M. Desimone, *Macromolecules*, 2006, **39**, 3427–3434.
 - ³ Data derived from: <http://polymerdatabase.com/polymers/polypropylmethacrylate.html> (last viewed August 8th 2020).